ternatively be considered as a +0.009 Å extension of the Fe–N_2 bond and a −0.009 Å contraction of the Fe–N_4 bond away from a mean equilibrium distance. A change of bond length of this order is beyond the resolving power of protein X-ray techniques and perhaps of the EXAFS method.[14]

From the sum of the energies of the occupied molecular orbitals for different extensions of Fe–N bond lengths one can make an approximate estimate of the distortion energy needed to cause the small ±0.009 Å Fe–N bond length change. This energy turns out to be ~100 cal/mol. Whatever the source of the distortion energy may be, it appears that such small distortions are less than kT at room temperature, so that near room temperature the porphyrin system might sample a number of such thermally accessible, slightly distorted conformations.[15] In the ENDOR measurements[1] that we have tried to interpret in this work, the temperature involved was ~2 K, so that the porphyrin system can be frozen into a particular configuration with different Fe–N bond distances, leading to the observed difference in $^{14}N_2$ and $^{14}N_4$ hyperfine constants. Thus, while our investigations do not rule out other possible sources for this observed difference, they do suggest that a difference in Fe–N_2 and Fe–N_4 bond lengths at low temperatures is a reasonable source.

Conclusions

The analysis carried out here has shown that the side chains of the protoporphyrin have a rather small influence on the unpaired electron densities at the pyrrole nitrogen atoms. The smallness of this effect on the pyrrole nitrogen atom leads us to expect even smaller influence of these side chains on the hyperfine properties[2,6] at the Fe nucleus and at the nuclei on the fifth and sixth ligands. This conclusion thus provides a justification for replacing the side chains in the porphyrin ring by hydrogen atoms when overall hyperfine properties of the inner nuclei of heme are under investigation as was done in earlier work.[2-4]

In view of the inability of the perturbations due to the side chains of the pyrrole ring to provide an explanation for the observed difference in $^{14}N_2$ and $^{14}N_4$ hyperfine constants, one has to look into other sources for this difference. One such possibility that has been explored here is a difference in the relative geometry of the nitrogens N_2 and N_4 (N_1 and N_3) with respect to the Fe. It is shown that a difference between diagonally opposite Fe-N bond lengths of only 0.018 Å can explain the observed[1] hyperfine differences in metmyoglobin. This difference in Fe–N bond lengths could perhaps originate from a difference in the interactions of the various pyrrole rings with protein groups. Alternatively, this difference in Fe–N_1 and Fe–N_3 (Fe–N_2 and Fe–N_4) bond distances could be an intrinsic property of the protoporphyrin IX unit. The results of X-ray measurements on five-ligand heme systems[16] without the protein chain are inconclusive in this respect. ENDOR measurements on single-crystal hemin and other halogen derivatives would be useful in throwing light on this question.

Acknowledgment. This work was supported by grants from the National Institutes of Health, HL-15196 (T.P.D.) and AM-17884 (C.P.S.).

Registry No. Nitrogen, 7727-37-9.

(14) P. Eisenberger, R. G. Shulman, G. S. Brown, and S. Ogawa, *Proc. Natl. Acad. Sci. U.S.A.*, **73**, pp 491–495 (1976).
(15) R. H. Austin, K. W. Beeson, L. Eisenstein, H. Frauenfelder, and J. C. Gunsalus, *Biochemistry*, **14**, 5355–5373 (1975).
(16) D. I. Koenig, *Acta Crystallogr.*, **18**, 663–672 (1965); S. C. Tang, S. Koch, C. C. Papuefthymiou, S. Foner, R. B. Fraenkel, J. P. Ibers, and R. H. Holm, *J. Am. Chem. Soc.*, **98**, 2414–2434 (1976).

Alterdentate Ligands: Determination of the Energy Barrier for Intramolecular Metal Ion Exchange in Complexes of Ninhydrin and Alloxan Radical Ions with Zn^{2+}, Mg^{2+}, Cd^{2+}, and Y^{3+}

C. Daul, E. Deiss,[1] J.-N. Gex, D. Perret, D. Schaller,[2] and A. von Zelewsky*

Contribution from the Institute of Inorganic Chemistry, University of Fribourg, Perolles, CH-1700 Fribourg, Switzerland. *Received April 11, 1983*

Abstract: The anionic radical ligands derived from ninhydrin (I) and from alloxan (II) form complexes with the closed-shell metal ions Mg^{2+}, Ca^{2+}, Zn^{2+}, Cd^{2+}, Y^{3+}, and La^{3+}. The radicals are generated in the cavity of an ESR spectrometer by an electrochemical method in dimethylformamide solutions of the corresponding metal perchlorates. Coordination of a metal ion in one of the chelating sites A or A′ (III and IV) reduces the symmetry of the paramagnetic species from C_{2v} in the free ligand to C_s in the complex. The splitting pattern due to the ligand protons (and ^{14}N nuclei in the alloxan radical complexes) is therefore, in general, different in the complexes as compared with the free ligand. Some of the metal complexes (Ca^{2+}, La^{3+}) show nevertheless an apparent C_{2v} symmetry of the ligands. This is interpreted in terms of a rapid intramolecular exchange from site A to A′. In other cases this intramolecular exchange gives rise to selective line broadening in the ESR spectra. The exchange rate can be determined by using a two-site jump model. The observed exchange rate constants are in the range $k = 5 \times 10^4$ s^{-1} to $k = 2 \times 10^7$ s^{-1}. Activation parameters are determined from the temperature dependence of the ESR spectra. These kinetic parameters for the exchange process suggest an associative mechanism for the ninhydrin radical and a dissociative mechanism for the alloxan radical. The series of metal ions with increasing intramolecular exchange rate is the same as that for water exchange in hydrated ions. INDO calculations and a molecular mechanics model indicate an out-of-plane motion of the metal ion on its pathway from site A to A′.

Alterdentate ligands offer, by definition, at least two equivalent sites for the binding of a metal ion.[3] Two ligands of this class are the radical anions of ninhydrin (I) and alloxan (II).[4]

Both ligands have in their uncoordinated forms C_{2v} symmetry, rendering the two pairs of protons (H^1/H^4 and H^2/H^3) in ninhydrin and the two NH groups in alloxan equivalent. This symmetry is mirrored in the ESR spectra of the free-radical anions,[5]

(1) Eidg. Institut für Reaktorforschung, CH-5303 Würenlingen, Switzerland.
(2) Sandoz AG, CH-4056 Basel, Switzerland.
(3) von Zelewsky, A. *Inorg. Chem.* **1981**, *20*, 4448.
(4) Schaller, D.; von Zelewsky, A. *J. Chem. Soc., Chem. Commun.* **1979**, 948.

0002-7863/83/1505-7556$01.50/0

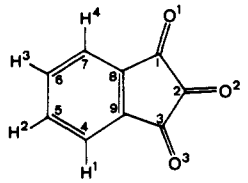

I

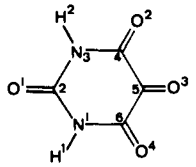

II

where 9 lines (a triplet of a triplet) are observed in the case of ninr[6] and 15 lines (a triplet of a quintet) in the case of allr. The radical anions can chelate metal ions at two different, but equivalent, sites, namely A and/or A′ in III and in IV, which makes them belong to the class of isoalterdentate ligands.[3]

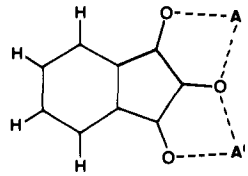

III

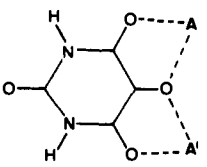

IV

In III and IV, only the molecular skeleton is depicted. The ligands contain, in addition to the π-electrons indicated in (I) and (II), a single unpaired electron delocalized over 12 centers in ninr and over 10 centers in allr.

When a metal ion occupies one site, say A only, the symmetry of the complex is C_s if the metal is coplanar with the ligand atoms. The formerly equivalent atoms become inequivalent. The ESR spectrum of III should now consist of $2^4 = 16$ lines and $3^2 \cdot 2^2 = 36$ lines in the case of IV if the metal introduces no new hyperfine splitting and ^{13}C satellites are neglected. Exchange of one coordinated metal ion from site A to A′ can, in principle, occur by inter- or intramolecular mechanisms. In the former case the metal dissociates from site A, and another or the same metal ion reenters to coordination site A′. In the latter case the metal remains coordinated along the exchange pathway from A to A′. The positional properties, e.g., coupling constants, of the pairs of nuclei in the ligand are modulated at the frequency of the exchange.[7] For several metal ions this exchange has just the right frequency to allow the observation of its effect on the hyperfine pattern of the ESR spectra of the radical complexes. In the present communication we report the kinetic parameters for several exchanging systems and we discuss possibilities for exchange pathways in the complexes.

Experimental Section

The radical complexes were generated inside the cavity using an electrochemical method described earlier.[8] For temperature variation a cell of the Allendoerfer type was employed.[9] For measurements in dimethylformamide (DMF) as a solvent, DMF-solvated metal perchlorates were used.[10] ESR spectra were measured on a Varian E4 spectrometer, equipped with a standard temperature control unit. The temperature was calibrated with a platinum resistance thermometer. Calculations were carried out on either a MINC 11/03 or an IBM 370-145 of the computer center of the University of Fribourg.

Results and Discussion

ESR Spectra of the Free-Radical Ligands. In aprotic solvents no complications due to protonation occur. Thus, for the radical anion of ninhydrin (ninr) in DMF with tetraethylammonium perchlorate (TEAP) as conducting electrolyte, a simple spectrum (Figure 1) consisting of 9 lines, i.e., a triplet of triplets, is observed by use of an electrochemical generation method. Russel[5] has given the ESR spectra obtained in aqueous solutions at different pH values. Despite the fact that Zn was used as a reducing agent, the spectrum of the free ligand has been obtained, because Zn^{2+} is strongly complexed by OH^- in basic solutions. The "low-pH" spectrum reported by Russel is similar to the DMF spectrum but the difference of the two coupling constants is larger (Table Ia). We have observed ESR spectra very similar to the one reported by Russel in neutral aqueous solutions of ninhydrin with $NaClO_4$ as conducting electrolyte obtained by cathodic reduction. The lines are narrow in these spectra (peak to peak width <8 μT) and an assignment to the nonhydrated form of the ninr radical is therefore most probable. The two coupling constants for the protons H^1/H^4 and H^2/H^3 (III) are not very different, and a definite assignment is therefore not easily possible. This assignment is, however, not crucial for the later discussion. The total width of the spectrum is only about 400 μT (in DMF or H_2O), indicating that the sum of the spin populations at the carbon atoms with H substituents is approximately 15%.[11] Eighty-five percent of the unpaired spin is delocalized over the remaining C centers and the oxygen atoms. This is in good agreement with the results of a spin-unrestricted INDO[14] calculation (Table IIa) which

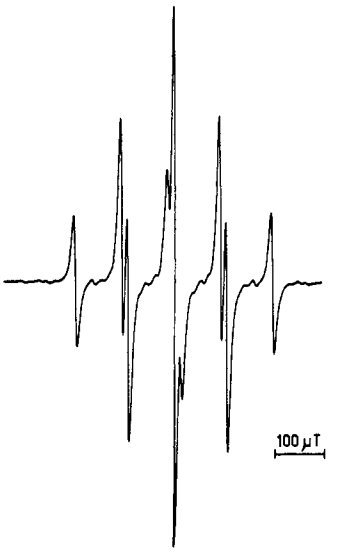

Figure 1. ESR spectrum of electrolytically generated ninr in DMF at room temperature.

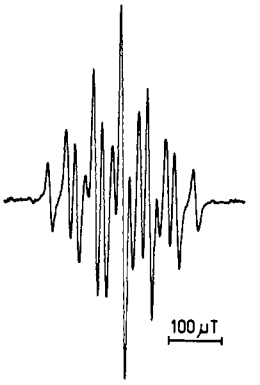

Figure 2. ESR spectrum of electrolytically generated allr in DMF at room temperature.

(5) Russel, G. A.; Young, M. C. *J. Am. Chem. Soc.* **1966**, *88*, 2007.
(6) The radical anions of ninhydrin (I) and alloxan (II) are designated by ninr and allr, respectively.
(7) Wertz, J. E.; Bolton, J. R. "Electron Spin Resonance"; McGraw-Hill: New York, 1972; pp 207–214.
(8) Richter, S.; Daul, C.; von Zelewsky, A. *Inorg. Chem.* **1976**, *15*, 943.
(9) Allendörfer, R. D.; Martinek, G. A.; Bruckenstein, S. *Anal. Chem.* **1975**, *47*, 890.
(10) Schneider, W. *Helv. Chim. Acta* **1963**, *46*, 1842.
(11) Using McConnell's relation (*J. Chem. Phys.* **1958**, *28*, 107).
(12) Bolton, W. *Acta Crystallogr.* **1965**, *18*, 5.
(13) Bolton, W. *Acta Crystallogr.* **1964**, *17*, 147.

Table I. ESR Parameters and Exchange Rate Constants of the Ninhydrin and Alloxan Radical Anions and Their Metal Complexes at Various Temperatures in DMF

metal	T/°C	coupling constants/μT a_{H^1}	a_{H^4}	a_{H^2}	a_{H^3}	a_M/μT	line width, μT	exchange rate constant, k/s^{-1}	remarks
				a. Ninhydrin[a]					
free ligand	25	104	104	92	92	-	8	-	c
Ca^{2+}	25	90	90	79	79	-	7	-	c, d
$^{111}Cd^{2+}/^{113}Cd^{2+}$	25	96	96	70	70	956/1000	9	-	c, d
$^{89}Y^{3+}$	25	94	94	67	67	42	8	-	c, d
$^{139}La^{3+}$	25	93	93	71	71	188	9	-	c, d
$^{67}Zn^{2+}$	100	121	73	96	48	145	9	-	d
Zn^{2+}	21	122	74	96	48		8	4.83×10^5	b
	39	121	73	95	47		8	7.0×10^5	
	48	121	73	95	47		8	1.4×10^6	
	50	121	73	96	48		8	2.05×10^6	
	67	121	73	95	47		7	4.1×10^6	
	75	121	73	95	47		10	4.5×10^6	
	100	121	73	96	48		9	6.1×10^6	
Cd^{2+}	22	123	73	95	46		9	3.5×10^6	b
	39	123	73	96	47		8	5.7×10^6	
	57	122	72	96	46		8	1.4×10^7	
	77	123	73	96	47		9	1.97×10^7	
Mg^{2+}	40	120	70	100	46		10	4.7×10^5	
	60	120	70	99	49		10	8.2×10^5	
	80	119	69	97	49		9	2.1×10^6	
	100	120	70	97	51		11	3.4×10^6	
				b. Alloxan[e]					
free ligand	25	33	33	48	48	-	8	-	c
Ca^{2+}	25	50	50	32	32	-	8	-	c, d
$^{111}Cd^{2+}/^{113}Cd^{2+}$	25	60	60	22	22	768/804	10	-	c, d
La^{3+}	25	54	54	27	27	191	9	-	c, d
$^{67}Zn^{2+}$	130	62	62	17	17	135	-	-	c, d
Zn^{2+}	25	84	43	39	0	-	8	8.7×10^4	b, f
	50	84	42	40	0	-	8	2.19×10^5	
	65	84	41	38	0	-	7	4.8×10^5	
	75	84	41	38	0	-	7	8.0×10^5	
	92	83	41	37	0	-	8	1.89×10^6	
	110	83	41	37	0	-	8	4.9×10^6	f
Mg^{2+}	50	81	40	40	8	-	8	5.9×10^4	
	70	78	39	42	8	-	9	1.12×10^5	
	80	80	39	40	9	-	7	1.85×10^5	
	100	78	39	40	9	-	7	4.0×10^5	
	120	76	38	39	9	-	7	1.09×10^6	
Y^{3+}	50	86	45	38	0	61	6	2.4×10^6	f
	70	86	45	36	0	60	6	2.9×10^6	
	90	84	45	35	0	59	6	6.4×10^6	
	110	84	45	34	0	57	6	1.3×10^7	
	130	64	64	16	16	55	7	-	d

[a] Assignment of the proton coupling constants has not been attempted. a_{H^1} and a_{H^2} are related to a_{H^4} and a_{H^3} by symmetry. [b] The fitting of the selectively broadened spectra were carried out by using nonenriched Zn complexes. In the case of the Cd complex only the central part of the spectrum was used for the fitting procedure. Metal coupling constants for this nucleus are therefore not obtained by this method. [c] From Schallei, D., Ph.D. Thesis, University of Fribourg, Fribourg, Switzerland. Calculations were made by using a Varian 620/L computer (program 994005-00C). [d] Fast exchange limit. [e] Assignment of values to atoms was not attempted: only a_{H^1} and a_{N^1} are related to a_{H^2} and a_{N^3}, respectively, by symmetry. [f] Poor calculations because the exchange is near the fast or the slow limit.

indicates that the spin density is mostly confined to the oxygen atoms of the radical anion. The spin densities on atoms showing hyperfine splitting are small and in most cases negative. An accurate prediction of the observed coupling constants can therefore not be expected.

The ESR spectrum of alloxan radical anion (allr) consists of 15 lines (Figure 2), as theoretically expected for two equivalent ^{14}N nuclei and two equivalent protons. The coupling constants are given in Table Ib and the results of the INDO calculations in table IIb. The total width of the spectrum is only 258 μT, in agreement with the results of the INDO calculations.

ESR Spectra of Metal Complexes: Qualitative Discussion of Exchange Effects. Striking effects occur in the ESR spectra of these radical ligands in the presence of metal ions, even in the case when the metal nuclei do not generate new hyperfine lines. Figure 3A shows the ESR spectrum of ninr in the presence of an excess of Zn^{2+} in DMF at room temperature. The lines 2,2′ and 3,3′ are strongly broadened, whereas 1,1′ and 4,4′ remain narrow. The intensity ratio of the lines 1 and 5 has dropped from 1:4 in the free ligand to 1:2 in the complex. Changing the temperature to 100 °C, where the radical can still be observed for extended periods (1 h), yields the spectrum shown in Figure 3B. The lines 2,2′ and 3,3′ have narrowed considerably, yielding a spectrum similar to that of the free ligand, though it shows significantly different intensity ratios. This behavior is interpretable by assuming a two-site jump process,[15] corresponding to an exchange of Zn^{2+} from coordination site A to A′ (III). The stick diagram for this exchange process is depicted in Figure 4.

It is clearly seen that the lines 2,2′ and 3,3′ at the intermediate positions are modulated by an amount corresponding to $2\Delta a$ (where $\Delta a = a_{H^1} - a_{H^2}$), whereas part of line 5, namely the

(14) QCPE program 389, rewritten in double precision and adapted to our IBM 370-145 computer.

(15) Bolton, J. R.; Carrington, A. *Mol. Phys.* **1962**, *5*, 161. deBoer, E.; Mackor, E. L. *J. Am. Chem. Soc.* **1964**, *86*, 1513. Freed, J. H.; Fraenkel, G. K. *J. Chem. Phys.* **1962**, *37*, 1156.

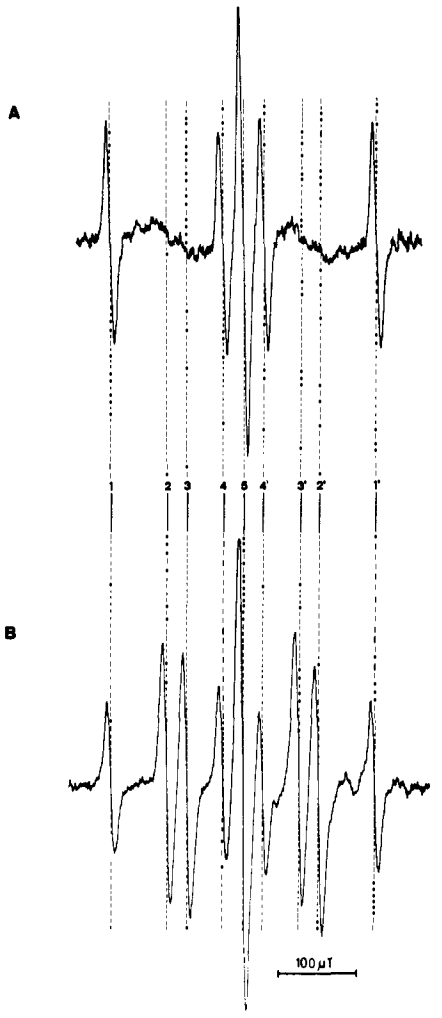

Figure 3. ESR spectra of $Zn(ninr)^+$ in DMF: (A) at 22 °C; (B) at 100 °C.

components yielding half of its intensity, is modulated by $4\Delta a$. The other components of line 5 and lines 1,1′ as well as 4,4′ do not shift their positions. According to Freed and Fraenkel,[15] the broadening of the lines is proportional to the square of the modulation amplitude. This means that the broad component of the central line 5 is four times as wide as lines 2,2′ and 3,3′. Raising the temperature increases the exchange frequency, which yields narrower lines. At 100 °C, the lines 3,3′ and 4,4′ are again clearly resolved, but they have not yet reached their full amplitude. The central line 5 has reached only 2.3 times the amplitude of 1,1′ since the broadening effect is still very strong. The slow-exchange limit cannot be reached either, because at lower temperatures the ESR signals become very weak. This is most probably due to a more exergonic disproportionation reaction at lower temperatures.

Table II. SCF-INDO Spin Densities

atom	spin density per atom			
	s	p_x	p_y	p_z
		in ninr[a]		
O^2	0.0117	−0.0013	0.0040	0.5062
C^2	0.0032	−0.0061	0.0052	0.0910
C^1/C^3	−0.0060	−0.0029	−0.0078	−0.0637
O^1/O^3	0.0055	0.0013	0.0022	0.2557
C^8/C^9	−0.0006	0.0000	−0.0001	−0.0067
C^4/C^7	0.0005	0.0003	0.0004	0.0135
H^1/H^4	−0.0006			
C^5/C^6	0.0000	−0.0001	−0.0001	0.0025
H^2/H^3	−0.0002			
		in allr[b]		
O^3	0.0129	−0.0025	0.0044	0.5544
C^5	0.0042	0.0065	0.0049	0.1285
C^4/C^6	−0.0049	−0.0005	−0.0064	−0.0223
O^2/O^4	0.0042	0.0022	0.0005	0.1888
N^1/N^3	−0.0026	−0.0013	−0.0007	−0.0243
H^1/H^2	0.0002			
C^2	0.0000	−0.0003	0.0006	−0.0006
O^1	0.0008	0.0002	0.0004	0.0333

[a] Geometry from ref 12. [b] Geometry from ref 13.

$$2Zn(ninr)^+ \rightleftarrows nin + Zn(nin^{2-}) + Zn^{2+} \qquad (1)$$

The hypothesis of a disproportionation reaction rests mainly on the observation that the electrolysis of the solution can be stopped once a sufficiently high concentration of the radical has been obtained. The radical concentration than changes in a nearly reversible manner with temperature, increasing strongly with increasing temperature.

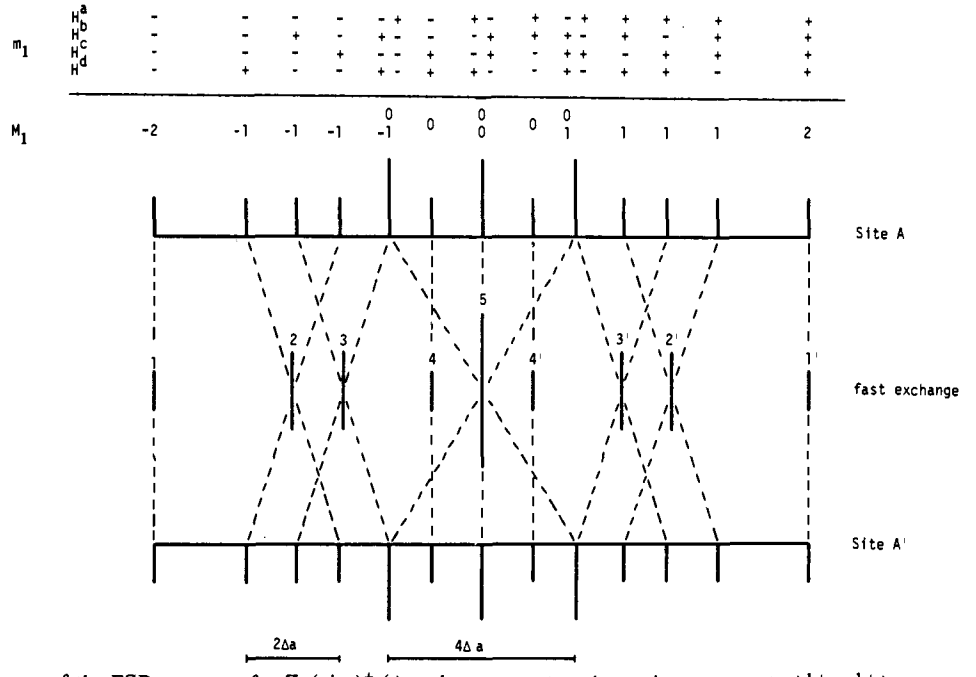

Figure 4. Stick diagram of the ESR spectrum for $Zn(ninr)^+$ (+ and − represent nuclear spin components $+^1/_2$, $-^1/_2$).

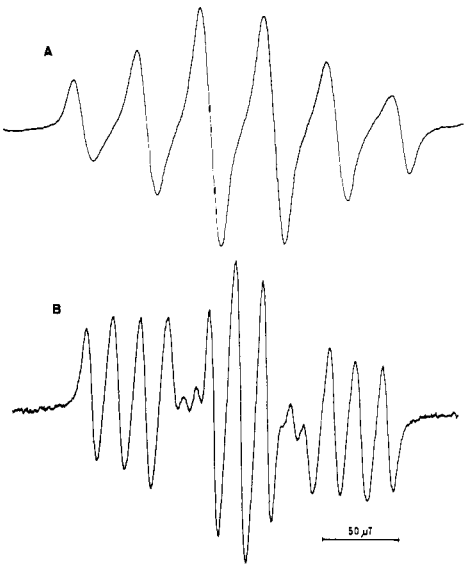

Figure 5. ESR spectra of $Zn(allr)^+$ in DMF: (A) at 25 °C (B) at 120 °C.

Similar effects of selective line broadening are observed with ninr and other closed-shell ions (vide infra). Exchange processes are also observed using the alterdentate ligand allr (IV). With this ligand the slow-exchange limit is almost reached in the Zn complex at 25 °C (Figure 5A). The fast limit is not yet completely attained at 120 °C (Figure 5B). The stick diagram depicting the modulation of the hyperfine lines is shown in Figure 6. It is seen that many lines are modulated by the exchange process but the modulation amplitude is strongly different for the various components. Other metal ions, i.e., Cd^{2+}, Mg^{2+}, Ca^{2+}, Y^{3+}, and La^{3+} also form complexes that undergo exchange reactions. Those having isotopes with nuclear spin show additional hyperfine structure of the metal nuclei (vide infra).

Mechanistic Aspects. The first problem to be discussed is the question whether the exchange of the metal ion from site A to A′ in the alterdentate ligands is an *intramolecular* or an *intermolecular* process. The most clear-cut proof for the intramolecular mechanism is the observation of a metal hyperfine structure in cases where the metal ion has a magnetic isotope. This is observed, e.g., in the case of the Cd^{2+} complex, where the two isotopes ^{111}Cd and ^{113}Cd ($I = {}^1/_2$, natural abundance 12.75% and 12.26%, respectively) give rise to hyperfine satellites. Although the spectra for the complexes $Cd(ninr)^+$ and $Cd(allr)^+$ are already near the fast-exchange limit (Figure 7) at room temperature, the metal hyperfine splitting is fully preserved. This can only be understood if it is assumed that the metal nucleus remains attached to the ligand during the exchange process; i.e., it is an *intramolecular exchange*. If the exchange were intermolecular, i.e., a metal ion leaves site A and another one enters at site A′, the hyperfine information would be lost.

The same result is obtained with enriched ^{67}Zn, which also shows hyperfine splitting from the metal nuclear spin at high temperature near the fast-exchange limit (Figure 8). Several other examples of metal hyperfine splittings have been observed. The data are given in Table I and a series of spectra are available in the supplementary material. Other evidence in favor of the intramolecular mechanism is the independence of the line broadening upon metal ion concentration.

For an intramolecular pathway two topologically different possibilities exist: (i) Motion of the metal ion is *in the molecular plane*. The symmetry along this reaction coordinate is

$$C_s \rightarrow C_{2v} \text{ (transition state or intermediate)} \rightarrow C_s$$

It is either a double- or a triple-minimum pathway, the latter if the linear arrangement corresponds to an intermediate. (ii) Motion of the metal ion is *out of the molecular plane*. The symmetry along this reaction coordinate is

$$C_s \rightarrow C_1 \rightarrow C_s \rightarrow C_1 \rightarrow C_s$$

Two degenerate pathways exist in this case. The two possibilities, (i) and (ii), can be understood by inspection of Figure 9. In the first case the out-of-plane angle θ remains zero during the exchange process, whereas in the second case it is only zero in the two equilibrium positions A and A′ but different from zero in the transition state/intermediate. It should be noted that the plane of symmetry in the initial and in the final states is orthogonal to the plane of symmetry in the transition state/intermediate.

From a naive point of view it is pathway ii which is probably more favorable, since the bond between the central oxygen and the metal can be fully maintained during the exchange process

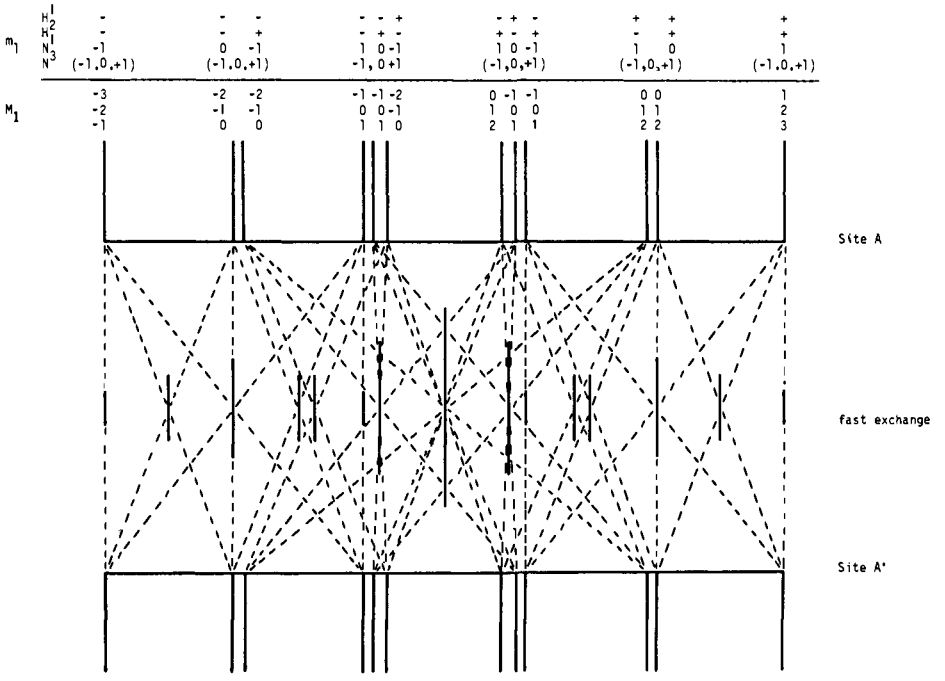

Figure 6. Stick diagram of the ESR spectrum for $Zn(allr)^+$. The simplification of the spectra at 25 °C (12 lines instead of 36) is due to $a_{N^3} \approx 0$. ESR spectra of $Y(allr)^{2+}$ show a similar effect (see Table III and related figures). "+" or "−" and (1, 0, −1) represent the spin components of hydrogen and nitrogen nuclei, respectively.

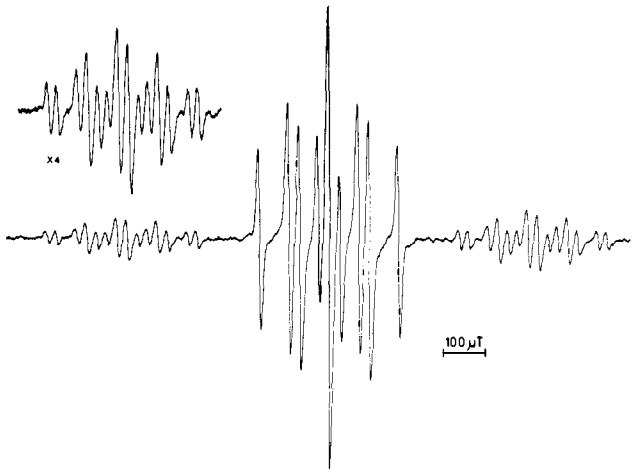

Figure 7. ESR spectrum of $Cd(ninr)^+$ in DMF at room temperature. The satellites are due to the isotopes ^{111}Cd and ^{113}Cd ($I = {}^1/_2$, natural abundance 12.75% and 12.26%).

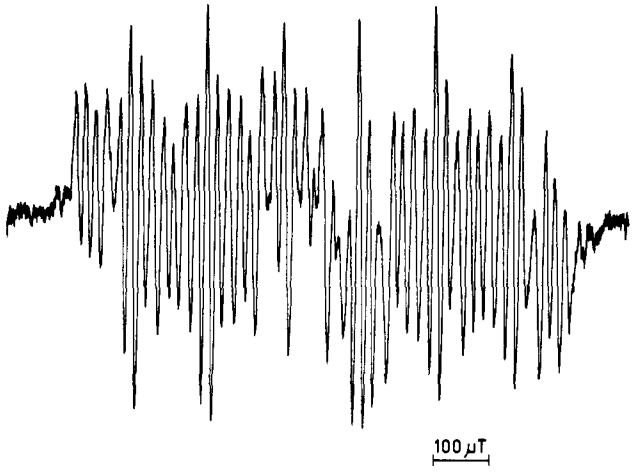

Figure 8. ESR spectrum of $^{67}Zn(allr)^+$ in DMF at 130 °C ($I = {}^5/_2$, enriched to ca. 90%).

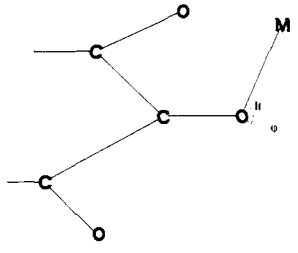

Figure 9. Angular coordinates for the intramolecular exchange process.

whereas in pathway i a rehybridization has to take place.

Determination of the Kinetic Parameters of the Metal Ion Exchange. The selective line broadening in the ESR spectra can be used for a quantitative determination of the exchange rates and the activation parameters. Heinzer[16] has developed a computer program that allows the determination of the relevant parameters by a nonlinear fitting procedure. The program was applied to the present spectra, which were digitalized by manual methods. The results are summarized in Table Ia,b. Some of the metal ions examined have too high exchange rates in order to give clearly observable line-broadening effects. This is the case for Ca^{2+} with ninr and allr and also for La^{3+} with both ligands. Although Ca^{2+} does not give rise to a metal hyperfine splitting, the formation of complexes is highly probable in view of the proton

(16) Heinzer, J. *J. Magn. Reson.* 1974, *13*, 124. Heinzer, J. *Mol. Phys.* 1971, *22*, 167.

Table III. Arrhenius Parameters for the Exchange Process

complex	exch. rate const at 298 K, s^{-1}	act. energy, kJ mol^{-1}	log of preexp factor	temp range, K
$Mg(ninr)^+$	2.3×10^5	33 ± 3	11.2 ± 0.5	313-373
$Zn(ninr)^+$	5.7×10^5	33 ± 4	11.5 ± 0.7	295-373
$Cd(ninr)^+$	3.9×10^6	28 ± 4	11.5 ± 0.6	295-350
$Mg(allr)^+$	1.3×10^4	44 ± 4	11.8 ± 0.5	323-393
$Zn(allr)^+$	4.4×10^4	50 ± 1	13.5 ± 0.2	338-365
$Y(allr)^{2+}$	3.3×10^5	41 ± 1	12.7 ± 0.1	343-383

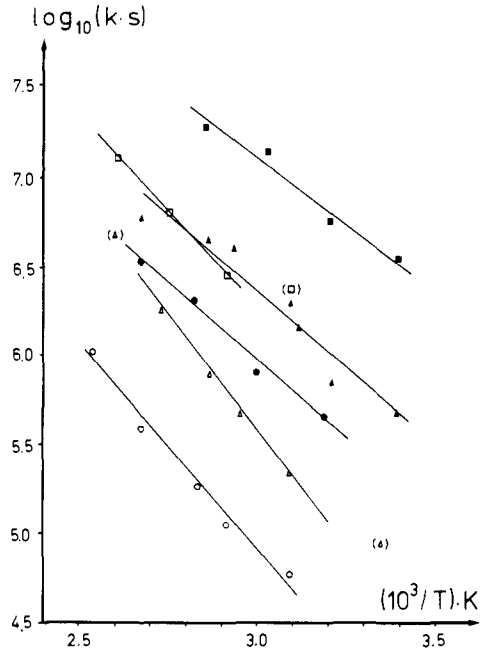

Figure 10. Arrhenius plots for the rate constant of the exchange process: (Δ) $Zn(allr)^+$; (○) $Mg(allr)^+$; (□) $Y(allr)^{2+}$; (▲) $Zn(ninr)^+$; (●) $Mg(ninr)^+$; (■) $Cd(ninr)^+$.

coupling constants, which are significantly different from the free-ligand values. In the case of La^{3+} the hyperfine splitting due to ^{139}La ($I = {}^7/_2$, 99.91%) is fully resolved in the complexes with both ligands. On the basis of the observed spectra, a lower limit of the exchange rate constant of $k_{ex} > 10^7\ s^{-1}$ at 25 °C can be estimated. The metal ions in $Cd(allr)^+$ and $Y(ninr)^{2+}$ also exchange too rapidly within the accessible temperature range. $Mg(ninr)^+$ on the other hand forms complexes that are not very stable. At low temperatures ($T < 80$ °C) at least two paramagnetic species are present, yielding nonsymmetric ESR spectra. The exchange rate at high temperatures can be estimated, and it is definitely slower when compared to $Zn(ninr)^+$. Approximate values for the exchange parameters are given in Table Ia.

For the complexes $Zn(ninr)^+$, $Cd(ninr)^+$, $Zn(allr)^+$, $Mg(allr)^+$, and $Y(allr)^{2+}$, a complete set of parameters could be determined for the intramolecular exchange process. The observable range of rate constants is ca. $5 \times 10^4\ s^{-1}$ to $2 \times 10^7\ s^{-1}$ (Table I). Since the spectra are relatively simple, good estimates for the coupling constants can be used as input data for the program. No particular difficulties were thus generally encountered in the fitting procedure. The only exception is the $Y(allr)^{2+}$ complex, where the hyperfine splitting of the metal nucleus has to be taken into account, because its coupling constant is small compared to the total width of the spectrum. Convergence is more difficult to reach in this case. In all cases simulated and measured spectra were compared visually in order to exclude fortuitous convergence. Table III gives the Arrhenius parameters and the rates at 298 K for the intramolecular exchange process (Figure 10).

The rate constants for intramolecular exchange are $Mg^{2+} < Zn^{2+} < Cd^{2+} < Ca^{2+}, La^{3+}, Y^{3+}$ for the ligand ninr and $Mg^{2+} < Zn^{2+} < Y^{3+} < Cd^{2+}, Ca^{2+}, La^{3+}$ for allr. This is the same order as that observed for water exchange in the first coordination

Table IV. *Activation Parameters $\Delta S^{\ddagger}$ and $\Delta H^{\ddagger}$ for the* Exchange Process

complex	$\Delta S^{\ddagger}$/ (J mol^{-1} K^{-1})	$\Delta H^{\ddagger}$/ (kJ mol^{-1})
Mg(ninr)$^+$	−42.9	29.4
Zn(ninr)$^+$	−61.2	20.6
Cd(ninr)$^+$	−41.5	22.7
Zn(allr)$^+$	+7.8	49.0
Mg(allr)$^+$	−0.7	51.5
Y(allr)$^{2+}$	−11.8	37.9
$Zn(H_2O)_6^{2+}$	+8.0[a]	36.0[a]

[a] From ref 17.

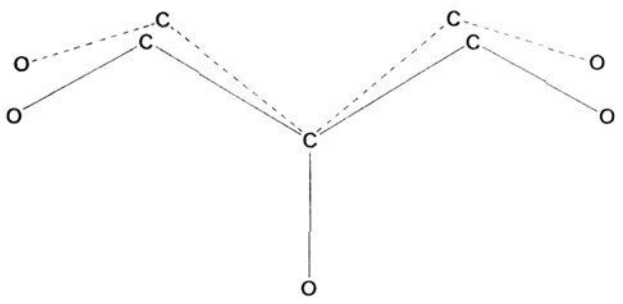

Figure 11. Geometry of the *vic*-triketone group in all (—) and nin[12,13] (---).

sphere[17] of these ions. The absolute values at room temperature are roughly a factor of 10 slower for Zn(ninr)$^+$ as compared to $Zn(H_2O)_6^{2+}$, and in Zn(allr)$^+$ the exchange is again a factor of 10 slower than in Zn(ninr)$^+$. Similar ratios are observed in the case of the other metal ions.

If the intramolecular exchange is compared with the exchange of an ordinary monodentate ligand like H_2O, some interesting relations can be observed. In Table IV the activation parameters for the intramolecular exchange and for the corresponding water exchange (literature data) are given. The latter is generally assumed to proceed via an dissociative mechanism. Even if the precision of the individual parameters, especially the activation entropies, are certainly not very high (error limits are not given, because they are difficult to estimate due to correlation among the two parameters), some general trends are observable. The allr complexes have entropies of activation which are similar to that of the aquo complex, and their slow rates are due to a relatively high enthalpy of activation. The contrary seems to be the case for the ninr complexes. Here the activation entropy is rather negative, whereas the enthalpy of activation is significantly smaller than in the allr complexes. Figure 11 gives the geometry of the chelating groups for nin and all, as determined by X-ray crystallography.[12,13]

Assuming no significant change in geometry upon reduction to the radical anions (or at least similar changes for both ligands), the ninr ligand could indeed be more likely to react via an associative mechanism than allr. In the transition state, one additional solvent molecule could be accommodated in the first coordination sphere, without too much crowding of ligand atoms. The allr ligand on the other hand has a smaller bite, and association of a solvent molecule is therefore less likely. The dissociation of one of the lateral oxygen ligands is, however, energetically a relatively unfavorable process.

Energy Surface Exploration. In order to study the reaction path from site A to site A′ during the exchange process, we have carried out two types of calculations. The first one is based on the CNDO/INDO[14] model and the second one uses a molecular mechanics model based on a simple multipole expansion of the calculated charge distribution.

In the first calculation we compute E_{tot}(INDO) for variable θ,ϕ angles (Figure 9) and minimize all the residual coordinates. For the sake of feasibility the metal ion is replaced by Li$^+$ and

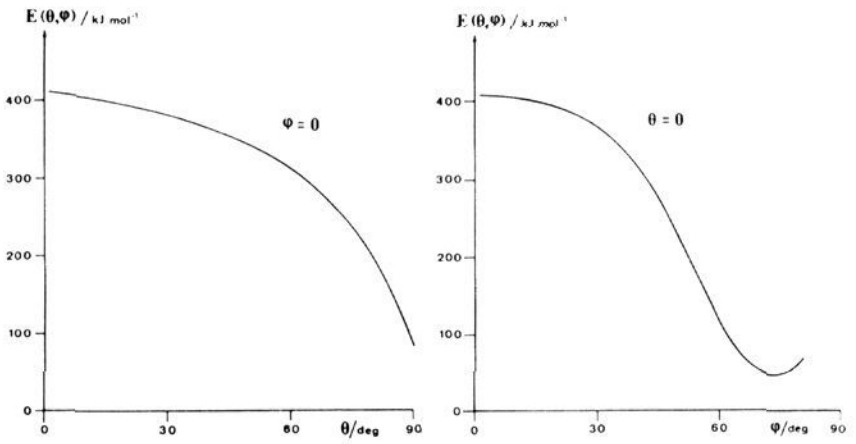

Figure 12. SCF-INDO total energy as a function of two possible reaction coordinates.

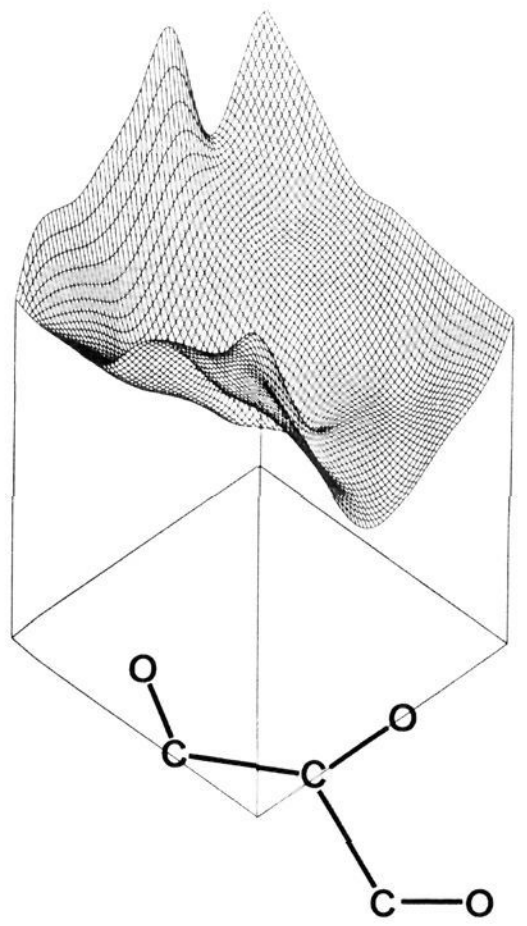

Figure 13. Energy surface for the metal exchange process, obtained by molecular mechanics.

no solvation is included. The energy function thus obtained can, at best, represent a general trend, and no significance should be given to the absolute values. The result of the calculation is presented in Figure 12. It is shown that if ϕ is varied from ϕ(equilibrium) to $-\phi$(equilibrium) the path of minimal energy corresponds to $\theta \neq 0$, i.e., to an "out of plane" mechanism. Indeed the geometry with $\theta = 0$ and $\phi = 0$ is a maximum in our energy calculation; thus the hypothesis of an "in-plane" mechanism has to be rejected on the basis of this calculation. Attempts to estimate the "true" transition-state geometry turned out to be unrealistic due to the absence of solvent molecules in our calculation. Computations including solvent molecules are unfeasible for reasons of excessive calculation time. In order to circumvent this problem we have decided to carry out a second calculation where we include solvent molecules in a simple way. Suppose that the potential energy surface $E = V(x_1,...x_{3N-6})$ can be represented satisfactorily by a molecular mechanics model. Thus, we expand the SCF (INDO) charge distribution of the radical anion into multipoles, up to dipoles, surrounded by a repulsive potential $\sim r^{-m}$ ($6 < m < 12$) and represent solvent molecules by dipoles in spherical cages. We then calculate $E(\theta,\phi)$ by minimization of all residual coordinates. Polarization effects are neglected in this approximation. The result of this calculation is presented in Figure 13. It shows that the reaction path from site A to site A′ corresponds again to an "out-of-plane" mechanism. The minimum energy path passes a saddle point and reaches a local minimum corresponding to $\theta = 90°$ and $\phi = 0°$, suggesting the existence

(17) Eigen, M. *Pure Appl. Chem.* **1963**, *6*, 97. Bennetto, H. P.; Caldin, E. F. *J. Chem. Soc. A* **1971**, 2198. Cotton, F. A.; Wilkinson, G. "Advanced Inorganic Chemistry", 4th ed.; Wiley-Interscience: New York, 1980; p 1188. Merbach, A. E. *Pure Appl. Chem.* **1982**, *54*, 1479.

of an intermediate with the metal ion normal to the ligand molecular plane, roughly above the central oxygen atom. This is approximately in agreement with conservation of hybridization at the central oxygen ligand. It is difficult to differentiate experimentally between the two mechanisms.

Conclusions

The exchange process of some closed-shell metal ions in the alterdentate radical ligands ninr and allr is a relatively fast intramolecular process. It represents an example for a molecular system in which a charged species can wander along a path of low potential energy without becoming detached from the parent structure. The presently investigated systems represent but the simplest situations, in which two symmetric minima exist on the energy hypersurface. Organized structures of higher complexity could extend the possibilities for such motion of ionic species considerably.

Acknowledgment. This work was supported by the Swiss National Science Foundation. We thank the Computer Center of the University of Fribourg for a generous grant of computer time.

Supplementary Material Available: Observed and simulated ESR spectra (Figures 14–44), most spectra used for the evaluation of the kinetic data, and the spectra of the rapidly exchanging complexes are given (28 pages). Ordering information is given on any current masthead page.

Nuclear Magnetic Resonance and Calorimetric Studies on the Solvation of Cryptand C221 and Its Na^+ and K^+ Complexes in Nonaqueous Solvents

Emmanuel Schmidt,[1] Jean-Michel Tremillon,[1] Jean-Pierre Kintzinger,[2] and Alexander I. Popov*[1]

Contribution from the Department of Chemistry, Michigan State University, East Lansing, Michigan 48824, and Institut Le Bel, Universite Louis Pasteur, 67000 Strasbourg, France.
Received April 15, 1983

Abstract: Carbon-13 and proton NMR as well as calorimetric measurements were used to study interactions of cryptand C221 with Na^+ and K^+ ions and with organic solvent molecules in a variety of nonaqueous solvents. The NMR spectra of the two alkali complexes in solution are quite different, indicating that the ligand exists in different conformations (as it does in the crystalline state). The ^{13}C spectra of free ligands in different solvents fall into two groups, designated here as A and B. Class A spectra are similar to those of the K^+·C221 complex while class B spectra approximate that of the Na^+·C221 complex. In the former case the spectra are believed to indicate a significant solvent molecule–ligand interaction. Calorimetric measurements show that while C221 forms a more stable complex with Na^+ than with K^+, the enthalpy of complexation in the latter case is more negative but the K^+ complex is entropy destabilized. The Na^+/K^+ selectivity strongly depends on the solvent and is especially pronounced in nitromethane solutions.

A number of previously reported studies have clearly shown that the stabilities of macrocyclic complexes are very significantly affected by physicochemical properties of the solvent in which the reaction takes place.[3-5] The role of the solvent becomes even more evident when we consider separately the enthalpy and the entropy of complexation.[3]

It is obvious, of course, that the extent of the cation–solvent interaction can have a very significant influence on the thermodynamics of complexation reactions. Other factors, however, may play an equally prominent role; in particular, the role of solvent–ligand interactions in complex formation seems to be somewhat neglected, although Hinz and Margerum indicated some years ago[6,7] that such interactions can have an important influence on the overall complexation reaction.

Recent studies by several investigators have shown that in some solvents crown ethers strongly interact with solvent molecules. In fact, solid solutes of 18-crown-6 with acetonitrile,[8] acetamide,[9] and nitromethane[10] have been isolated and, in the latter case, the structure of the complex, $18C6\cdot(CH_3NO_2)_2$, has been determined by X-ray crystallography. Clearly such interactions must also exist, to a greater or lesser extent, in solutions and must modify the complexing abilities of the macrocycles; they may, for example, alter the conformation of the macrocyclic ligand, rendering it either less or more capable of complex formation.

It has been stated recently that solvent–cryptand and solvent–cryptate interactions are weak in comparison with the solvent–cation ones and moreover that the former do not vary significantly from solvent to solvent.[11] It should be noted, however, that direct calorimetric measurements of Abraham et al.[12] showed that the enthalpy of transfer of cryptand C222 from water to methanol is +13.9 kcal mol^{-1} while for 18C6 it is +13.6 kcal mol^{-1}. These results clearly indicate not only that the enthalpy of solvation of macrocyclic ligands can be very substantial but also that it can vary drastically with the solvent.

It should be noted that in the vast majority of cases where the enthalpy and the entropy of macrocyclic complex formation were determined in nonaqueous solvents, the complexes were found to be enthalpy stabilized but entropy destabilized.[13] The magnitudes of the entropy changes, however, very much depend on the nature of the solvent. The desolvation of the cation and/or the ligand

(1) Michigan State University.
(2) Institut Le Bel.
(3) Shamsipur, M.; Rounaghi, G.; Popov, A. I. *J. Solution Chem.* **1980**, *9*, 701.
(4) Lin, J. D.; Popov, A. I. *J. Am. Chem. Soc.* **1981**, *103*, 3773.
(5) Cox, B. J.; Garcia-Rosas, J.; Schneider, H. *J. Am. Chem. Soc.* **1981**, *103*, 1384. Cox, B. J.; Schneider, H.; Stroka, J. J. *Ibid.* **1978**, *100*, 4746.
(6) Hinz, F.; Margerum, D. W. *J. Am. Chem. Soc.* **1974**, *96*, 4993.
(7) Hinz, F.; Margerum, D. W. *Inorg. Chem.* **1974**, *13*, 2941.
(8) Gokel, G. W.; Cram, D. J.; Liotta, C. L.; Harris, M. P.; Cook, F. L. *J. Org. Chem.* **1974**, *39*, 2445.
(9) Vogtle, F.; Muller, W. M.; Weber, E. *Chem. Ber.*, **1980**, *113*, 1130.
(10) DeBoer, J. A. A.; Reinhoudt, D. N.; Harkema, S.; vonHummel, G. J.; deJong, F. *J. Am. Chem. Soc.* **1982**, *104*, 4073.
(11) Gutknecht, J.; Schneider, H.; Stroka, *Inorg. Chem.* **1978**, *17*, 3326.
(12) Abraham, M. H.; Danil DeNamor, A. F.; Lee, W. H. *J. Chem. Soc., Chem. Commun.* **1977**, 892. Abraham, M. H.; Ling, H. C. *Tetrahedron Lett.* **1982**, *23*, 469.
(13) (a) References 3–5 and references listed therein. (b) Lamb, J. D.; Izatt, R. M.; Christensen, J. J.; Eatough, D. J. In "Coordination Chemistry of Macrocyclic Compounds"; G. A. Melson, Ed.; Plenum Press: New York, 1979; Chapter I.

0002-7863/83/1505-7563$01.50/0